



Green Synthesis and Characterization of Metal Oxide-cellulose Nanocrystals (MO-CNC)

DANILET VI M. MENDOZA^{1*}, MARIO M. ABESAMIS JR.¹ and MARILENE C. HIPOLITO¹

¹Department of Natural and Applied Sciences, College of Arts and Sciences Nueva Ecija University of Science and Technology General Tinio St., Cabanatuan City 3100, Philippines.

*Corresponding author E-mail: niletmendoza@yahoo.com

<http://dx.doi.org/10.13005/ojc/410122>

(Received: November 21, 2024; Accepted: January 20, 2025)

ABSTRACT

MO-CNCs were developed using rice straw, sugarcane bagasse, and corn straw as raw materials. The extracted CNCs were incorporated with different ratio of CuO and ZnO nanoparticles. Both nanosized spherical and rod-like structures of CNCs were obtained. Incorporation of MO nanoparticles produced the nanoparticle CNC matrix with prominent agglomeration. Bands were observed at around 400 to 600 cm^{-1} attributed to MO-CNC interaction. Incorporation of MO nanoparticles improved the thermal stability of CNC. The peak temperature obtained for the products were within the range of 308-360°C.

Keywords: MO-CNC, Biocomposite, Agro-residue, Cellulose nanocrystals, Nanomaterials.

INTRODUCTION

One of the most widely available renewable biopolymer on earth is cellulose. Over the years it remains to be one of the inexhaustible raw materials due to its wide variety of use. Recent advances were made for its modification to further increase its potential as raw material. This includes converting the cellulose into nano-sized particles which improves its strength and stiffness. In several studies, cellulose were modified by incorporating different compounds to add to its initial properties depending on the target application of the end product.

In the Philippines, region III is strategically located between Northern Luzon and the National

Capital Region. It is where the largest central plain in the country can be found. Thus, the main source of income of families in the region is farming. Despite of its being coined as the rice granary of the country, several crops aside from rice are being contributed by largely by the region. In terms of metric tons harvested for the year 2020, the top three crops are palay, sugarcane, and corn giving harvested yield equivalent to 3,635,147.59, 415,301.84, and 274,274.82 metric tons respectively. Several studies have been conducted to extract and isolate cellulose fibers from rice straw. The by-products or agro-residue in the harvesting and processing of sugarcane include bagasse and straw. Development of products out of sugarcane bagasse and straw have been explored such as its conversion to bioethanol



and textile. Despite of it being utilized, the increase in the volume of sugarcane production deemed it necessary to continuously find ways to utilize these by-products. As reported by the Philippine Statistics Authority, there was a 110.8% percent increase in the production of sugarcane during the third quarter of 2021 in comparison with the previous year. Sugarcane straw is composed of 32.4 to 44.4% cellulose while sugarcane bagasse is composed of about 40-50% cellulose. The Department of Agriculture Region Office III (DARFO3) launched a Corn Program. The Corn Program seeks to boost the production of high-quality corn and cassava for human consumption, animal feed, and industrial purposes, while also empowering farmers, raising their incomes, and enhancing their overall quality of life. This suggests that rise in corn production should be expected for the succeeding years. However, similar challenges encountered for rice straw being burned or left for soil fertilization occurs. Thus, other ways of utilizing corn stalks should be explored. Corn stalk is composed of about 32.73% cellulose.

Green synthesis of metal oxide cellulose nanocomposites have been attracting interests worldwide due to its beneficial industrial properties. These nanocomposites have been found to have antimicrobial properties against gram negative bacteria¹, can degrade dyes thru photocatalysis², anticancer activity³, cytotoxic activity^{4,5} and anticorrosive and antioxidant⁶. Thus, utilizing agro-residue to cellulose nanocomposites pose great advantages. The main aim of the project is to synthesize MO-CNC using the top three most abundant agro-residue in Region III as raw material and determine its characteristics.

MATERIALS AND METHODS

Sample Collection and Preparation

Samples were washed with distilled water to remove dirt. These were then cut into small pieces and placed in the oven at 105°C for 10 hours. It was then grinded using an osterizer. The oven drying and grinding steps were repeated until fine powder were obtained. The powder was then sieved under 60 mesh. Samples were kept in a dessicator for the extraction of cellulose.

Extraction of Cellulose Fibers

The method was adopted from previous

study¹. Dried plant powder samples were sieved under 60 mesh. Solvent extraction was performed in a Soxhlet apparatus using hexane as solvent with a ratio of 250 mL per 5g of the sample for 6 hours. Alkaline pretreatment followed. Screw cap glass bottles were used to contain a mixture of 2% sodium hydroxide (NaOH) and 10% solid load (1:10 w/v) subjected at 121°C for 30 min in an autoclave. After cooling, vacuum filtrated followed using grade 1 Whatman filter paper. The pretreated biomass was made neutral through washing with deionized water. Drying followed for 24 hours at 65°C using a hot air oven.

Cellulose Nanocrystals Synthesis

The obtained cellulose fibers were used as precursors for CNC synthesis. The process of Kumar *et al.*,⁷ was utilized for the acidic extraction of CNCs. The mixture of fibers and 64% (w/w) H₂SO₄ solution with 1:10 g/mL ratio was subjected to continuous stirring for 60 min at temperature of 40°C. The extraction was stopped by mixing 10-fold cold distilled water. The solution was then subjected for 15 min to successive centrifugation at 10,000-12,000 rpm. The sediments were then harvested and suspended in distilled water prior to dialysis to obtain a neutral pH. Centrifugation and sonication followed. Sonication of the CNCs was conducted in an ice bath for 10 min prior to storage at 4°C in the refrigerator.

MO-CNC nanocomposites preparation

Metal oxide cellulose nanocrystals were synthesized following the procedure developed by Azizi *et al.*,⁸. A solution of CNCs in deionized water and metal acetate dihydrate in ethanol were subjected to mixing using a magnetic stirrer. Weight ratio was varied and investigated. With gentle stirring at 80°C, the solution was added dropwise with 5M sodium hydroxide solution. Using centrifuge, different phases of metal oxide/CNC nanocomposites were separated. Distilled water was used to remove the by-products and unreacted CNCs. Drying for 1 h at 120°C followed to allow complete reaction of metal hydroxide to metal oxide.

Characterization of CNC and MO-CNC

Dimensions of the product was determined through the use of Transmission electron microscopy (TEM). This was done by a third party testing laboratory. Using a copper grid coated with a thin carbon film, a drop of the suspension (0.1 wt%) was

adhered. Drying followed prior to TEM analysis using 100kV accelerating voltage for better contrast.

The structural changes as to functional groups were investigated using a Shimadzu IRSpirit Fourier transform infrared spectroscopy–attenuated total reflectance (FTIR-ATR). About 4-5 h of drying of samples was conducted at 105°C prior to analysis. Less than 10 mg of the products were loaded for analysis.

Strength and degradation of the products were evaluated based on Thermogravimetric Analysis (TGA) using a Perkin Elmer STA 6000. Using a nitrogen atmosphere, the thermal behavior of the products were obtained. The heating rate of 10 °C/min from 30 to 900°C was utilized. This was done by a third party testing laboratory.

RESULTS AND DISCUSSION

Synthesis of MO-CNC

Cellulose fibers were extracted from all the samples. Dewaxing was done using hexane as solvent. This was followed by pretreatment using alkali solution. These steps were conducted to remove the wax, lignin and other covering of the samples to expose and extract the cellulose fibers.

The cellulose extracted were converted into cellulose nanocrystals via acid hydrolysis using sulfuric acid. The synthesized cellulose nanocrystals were then used for the development of MO-CNCs. Different ratio of metal oxide and cellulose nanocrystals were investigated and characterized. The ratio of the prepared MO-CNC are shown on Table 1. Same ratio was utilized for CNC from the three sources of cellulose.

Table 1: Ratio of metal oxide and CNC prepared

Sample	CuO	ZnO	CNC
1	1	2	1
2	2	1	1
3	1	2	2
4	2	1	2
5	1	1	1

Characterization of CNC and MO-CNC

The nanosized dimension of the products were revealed in the TEM analysis. Cellulose nanocrystals are characterized by their rod-like or spherical structures with varying width and length

depending on its synthesis. TEM images of the synthesized CNCs were shown in Figure 1.

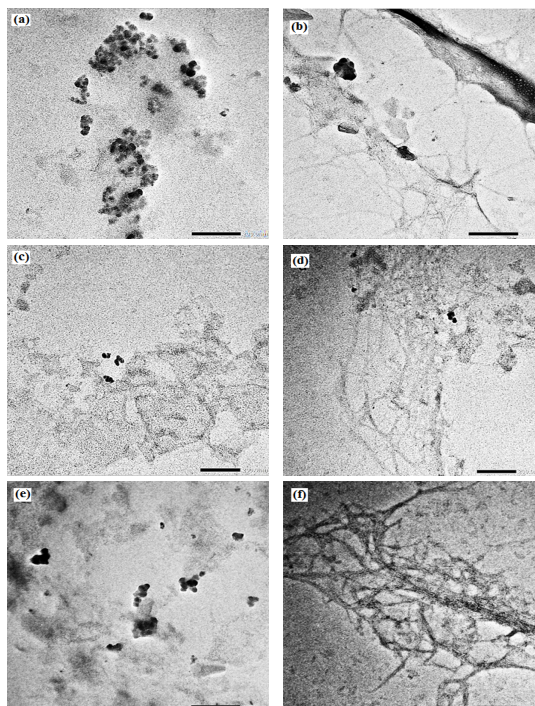


Fig. 1. TEM images at 200nm of synthesized (a) spherical CNC and (b) rod-like CNC from rice straw, (c) spherical CNC and (d) rod-like CNC from sugarcane bagasse, and (e) spherical CNC and (f) rod-like CNC from corn straw

As shown in Fig. 1, the synthesized CNCs has a mix of spherical and rod-like structures with diameter and width of less than 200nm respectively. These mixed structures were similar with CNCs obtained from previous studies^{9,10}. Formation of the spherical CNCs is due to ultrasonication¹¹. The study of Lu and Hsieh¹² revealed that spherical CNCs has mesopores that are absent in rod-like structures. Thus, the formation of spherical CNC greatly influence its thermal stability and physicochemical properties. Aggregation of CNCs are observed in the TEM images due to drying and redispersion of the samples in water that were done prior to imaging. More dispersed CNCs can be obtained from samples that were not dried as observed in the study of Kaushik *et al.*,¹³.

Metal oxide nanoparticles are characterized by spherical shapes in TEM. Upon incorporation of metal oxide nanoparticles to CNC, it was observed that the metal oxide nanoparticles were dispersed in the CNC matrix as shown in Figure 2.

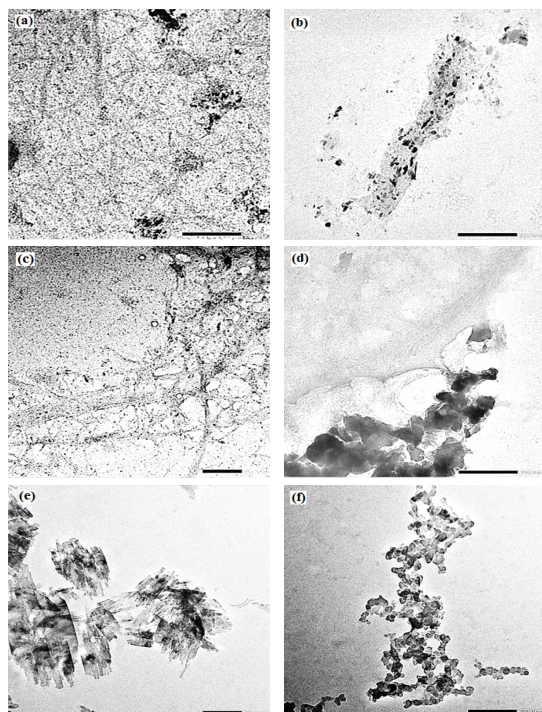


Fig. 2. TEM images of ZnO/CuO-CNCs at 200nm from (a) and (b) rice straw, (c) and (d) sugarcane bagasse and (e) and (f) corn straw

As can be gleaned from the figure, the smaller spherical metal oxide nanoparticles are

dispersed in both spherical and rod-like structures of the CNCs. Metal oxide nanoparticles have smaller size within the range of 20-50nm as compared to spherical CNC.

Structural changes in terms of functional groups in the cellulose nanocrystals upon incorporation of metal oxide were investigated by spectral analysis.

As shown in Fig. 3a for products from rice straw, the sharp peaks at around 1548 cm^{-1} and 1387 cm^{-1} in the ZnO NP may be attributed to asymmetric and symmetric C=O stretching of precursor zinc acetate. This is in congruence with the results of the study of Kwabena *et al.*,¹⁴ which suggest the occurrence of carboxylate groups due to low transformation rate. The appearance of peak for the ZnO/CuO-CNC at 1559 cm^{-1} may be attributed to both stretching and bending vibration of the bridged hydroxyl groups on the ZnO¹⁵. Characteristic peaks of ZnO NP at around 430 cm^{-1} were observed for both spectra of ZnO NP and ZnO/CuO-CNC^{16,17}. The band at 896 cm^{-1} is indicative of the beta-glycosidic linkage of cellulose monomers¹⁸. This band is present in both CNC and ZnO/CuO-CNC spectra. Another characteristic peak of cellulose present in both spectra include C-C stretching at around 1159 cm^{-1} . Same peaks were observed for ZnO-CNC synthesized from corn straw (Figure 3c).

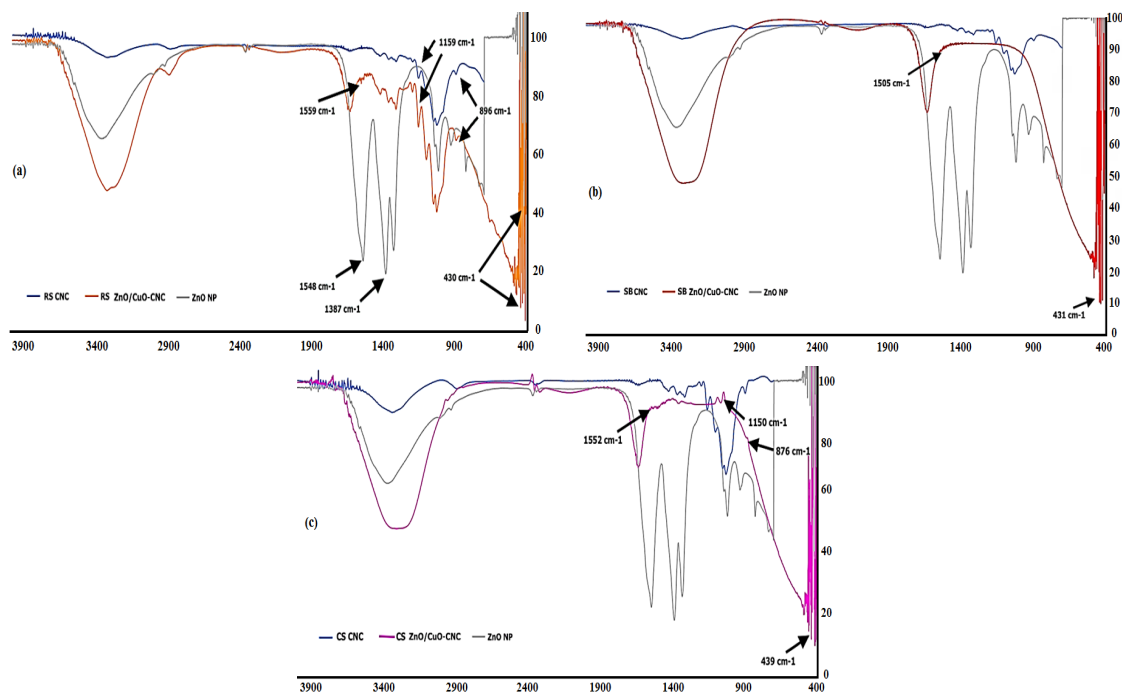


Fig. 3. FT-IR spectra of ZnO/CuO-CNC (higher ratio of ZnO) from a) rice straw, b) sugarcane bagasse, and c) corn straw showing prominent characteristic peaks of both cellulose and ZnO NP

For the products from sugarcane bagasse, the characteristic peak at 431 cm^{-1} of ZnO NP is also evident. However, the peak due to stretching and bending vibration of the bridged hydroxyl groups of the ZnO/CuO-CNC at 1505 cm^{-1} is barely noticeable. This implies that less ZnO NP is attracted to the CNC. Moreover, the peaks at around 896 cm^{-1} and 1159 cm^{-1} corresponding to beta-glycosidic linkage of cellulose monomers and C-C stretching respectively are also absent. This implies that the CNC from sugarcane bagasse upon incorporation of higher ratio of ZnO NP has been broken down.

As shown in Fig. 4, characteristic peaks of CuO NP occurs at around 460 cm^{-1} to 650 cm^{-1} . These are peaks attributed to Cu-O bond stretching¹⁹.

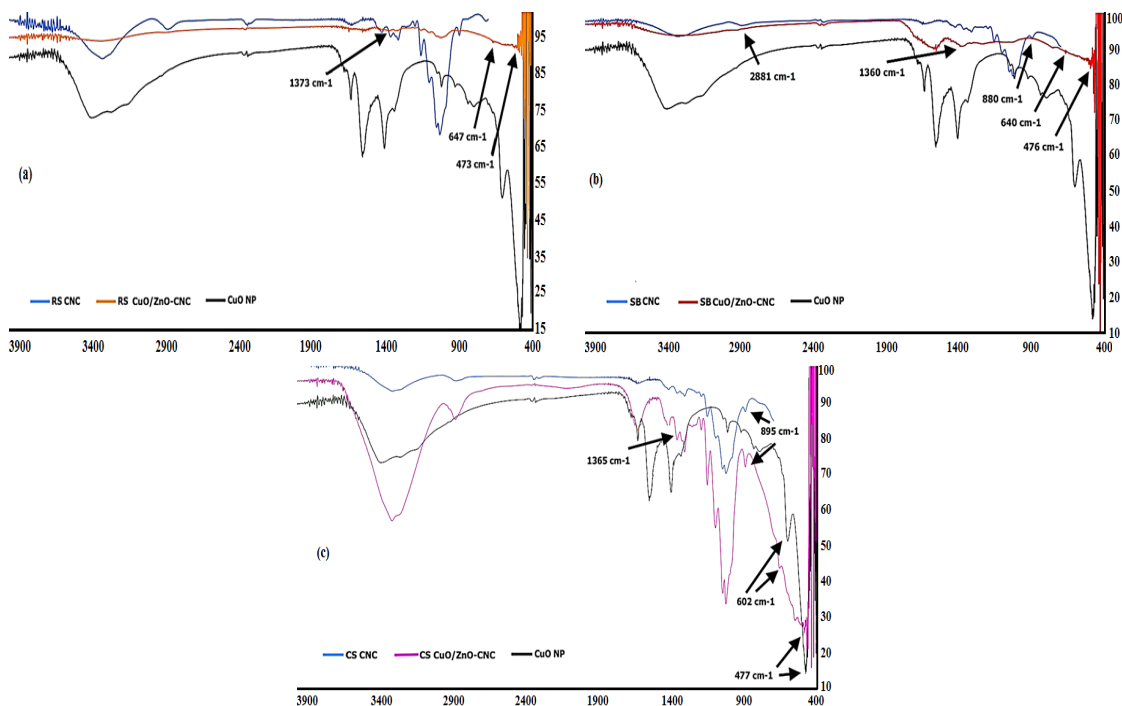


Fig. 4. FT-IR spectra of CuO/ZnO-CNC (higher ratio of CuO) from a) rice straw, b) sugarcane bagasse, and c) corn straw showing prominent characteristic peaks of both cellulose and CuO NP

Thermogravimetric analysis was conducted to evaluate the degradation profile due to weight loss of the products with increasing temperature. This is important in assessing the thermal stability of the products. Table 3 shows the TG-DTG data obtained. The greatest rate of change on the weight loss curve was implied by the peak temperature. Peak temperature range of $50\text{-}235^{\circ}\text{C}$. with accompanying weight loss within the range of $1\text{-}12\%$ may be attributed to the water molecules evaporation in the samples²⁰.

These peaks were observed in all CuO/ZnO-CNC synthesized. However, product synthesized from corn straw has more pronounced peaks (Fig. 4a). This also yielded a noticeable band indicative of the beta-glycosidic linkage of cellulose monomers at around 896 cm^{-1} . Interaction of the CuO and CNC can be seen through the band that occurs at around 1365 cm^{-1} which signifies the C-O stretching of the carboxylate ion next to hydroxyl groups attracted to CuO. Similar with the observations on the spectra of sugarcane bagasse ZnO/CuO-CNC, several peaks indicative of beta-glycosidic linkage of cellulose monomers and C-C stretching are absent (Fig. 4b). Hence, it can imply that incorporation of metal oxide nanoparticles to CNC from sugarcane bagasse can lead to its degradation.

The second peak temperature of the samples within the range of $320\text{-}360^{\circ}\text{C}$. corresponds to the pyrolysis of cellulose and hemicellulose that caused the drastic weight loss of the samples²¹. The third peak temperature at 526.38°C . for rice straw CNC and 620.93°C . for sugarcane bagasse may be attributed to its higher lignin content. Lignin has relatively higher pyrolysis temperature compared to cellulose which can reach up to 900°C .

Table 2: TG-DTG Data of MO-CNC products

Sample		Peak Temperature (°C)	Weight Loss (%)
Rice straw	Pure CNC	56.42	6.548
		323.4	72.305
		526.38	14.913
	CuO/ZnO-CNC 1:2:2	67.35	3.206
		342.97*	66.304
		57.44	6.523
	CuO/ZnO-CNC 1:1:1	315.27	65.11
		66.89	3.548
	CuO/ZnO-CNC 2:1:1	337.92	57.774
		62.07	7.432
	CuO/ZnO-CNC 2:1:2	277.29	14.904
		317.59	50.405
	CuO/ZnO-CNC 1:2:1	48.08	4
330.65*		41.14	
Sugarcane bagasse	Pure CNC	68.47	2.365
		350.49	64.201
		620.93	19.324
	CuO/ZnO-CNC 1:2:2	65.36	7.426
		359.33*	63.59
		67.9	1.357
	CuO/ZnO-CNC 1:1:1	344.67	44.599
		48.42	4.349
	CuO/ZnO-CNC 2:1:1	292.38	15.682
		328.91	29.592
	CuO/ZnO-CNC 2:1:2	63.65	3.114
		355.35*	62.659
	CuO/ZnO-CNC 2:1:2	59.48	7.086
343.1		54.31	
CuO/ZnO-CNC 1:2:1	75.75	56.32	
	349.02	10.465	
Corn straw	Pure CNC	51.1	11.356
		334.55	83.812
		70.42	2.774
	CuO/ZnO-CNC 1:2:2	283.06	11.867
		308.99	48.934
		44.39	4.872
	CuO/ZnO-CNC 1:1:1	314.09	52.529
		50.12	4.343
	CuO/ZnO-CNC 2:1:1	305.19	15.102
		346.75*	28.231
	CuO/ZnO-CNC 2:1:2	56.49	5.594
		343.72*	71.312
	CuO/ZnO-CNC 1:2:1	67.6	2.074
338.3		48.187	

*highest peak temperature of product for each raw material

Rice straw and sugarcane bagasse CNCs incorporated with lowest ratio of CuO nanoparticles increased its thermal stability to a peak temperature of 8-20°C. accompanied by lower weight loss percentage. CNC interacts with CuO electrostatically by means of its hydroxyl groups²². These interactions caused better dispersion and stabilization of the nanoparticle. These also serve as thermal barrier for the degradation of the

cellulose units which caused the increase in peak temperature. However, increasing further the ratio of CuO nanoparticles will cause its agglomeration instead of creating electrostatic interactions with CNC. Thus, lower peak temperature was observed for CNC with higher CuO ratio. Since the presence of lignin in corn straw CNCs is negligible, it can be deduced that there are greater number of free hydroxyl groups where CuO nanoparticles can

electrostatically interact. Thus, the corn straw CNC with higher ratio of CuO has higher peak temperature.

Rice straw CNC incorporated with higher ratio of ZnO nanoparticles has higher degradation temperature as compared to the pure CNC. The 7°C increase in peak temperature was also accompanied by a lesser weight loss percentage. These changes may be attributed to the addition of ZnO nanoparticles which formed stronger interactions with CNC, creating a thermal barrier for cellulose degradation²³. Thus, addition of larger amount of ZnO improves the thermal stability of the CNC. This was also supported by the high thermal stability of ZnO nanoparticles as reflected on its peak temperature of 278.89°C. with a low weight loss of 14.894%. Previous study of Zheng *et al.*,²⁴ also suggested that the use of ultrasonication also assisted the disruption of the cellulose network that causes the slight increase in thermal stability due to decrease in crystallinity. In the case of sugarcane bagasse and corn straw CNCs, the larger ratio of ZnO nanoparticles in the samples decreases the peak temperature due to its catalytic degradation properties. Previous studies also obtained similar findings^{25,26}. ZnO nanoparticles act as nanocatalysts at elevated temperature in the pyrolysis degradation of cellulose²⁷.

Thermogravimetric analysis of the MO-CNCs suggests that generally, an increase in the ratio of inorganic nanoparticles incorporation to CNCs causes an increase in thermal stability. The electrostatic interactions between the hydroxyl groups of the CNCs and the metal oxide nanoparticle creates a thermal barrier. However, properties of the nanoparticles also influence the thermal stability of the nanocomposite such as agglomeration and catalytic activity. Thus, these factors should be evaluated in developing MO-CNCs for health related applications if highly thermal resistant products are desired. The obtained peak temperature of the developed products were higher than previously reported

from literature even for the pure CNCs²⁸. Among the samples, sugarcane bagasse CuO/ZnO-CNC with 1:2:2 ratio of CuO/ZnO nanoparticles emerged with the highest peak temperature of 359°C. The previous study determined that acetylation of CNCs can further increase its thermal stability to 295°C. which makes its suitable for scaffolding. However, the observed peak temperature in the previous study was less than the peak temperature of the developed products even without acetylation. Thus, the high thermal stability of the developed products suggests its potential for component of scaffolding material for high temperature applications.

CONCLUSION

MO-CNC were synthesized using agro-residues. Nanosized spherical and rod-like structures of CNCs were obtained. Incorporation of MO nanoparticles produced the nanoparticle CNC matrix with prominent agglomeration. Bands were observed at around 400 to 600 cm⁻¹ attributed to MO-CNC interaction. Incorporation of MO nanoparticles improved the thermal stability of CNC. The peak temperature obtained for the products were within the range of 308- 360°C.

ACKNOWLEDGEMENT

The conduct of the study and development of the products were made possible by the support of the Department of Science and Technology-Philippine Council for Health Research and Development (DOST-PCHRD) thru DOST Region III- Central Luzon Health Research and Development Consortium (CLHRDC). Deep gratitude was also expressed to the Nueva Ecija University of Science and Technology (NEUST) administration for the utmost support during the conduct of the study and to the De La Salle University-Central Instrumentation Facility for facilitating the TEM analysis.

Conflict of Interest

The authors declare that there is no conflict of interest in this work with regards to publication.

REFERENCES

1. Saravanan, K.; Ilayaraja, M.; Muthukrishnan, P.; Ananthakrishnan, S.; & Ravichandiran, P., *J Indian Chem Soc.*, **2022**, 99(8), 100575.
2. Saravanan, K.; Ilayaraja, M.; Muthukrishnan, P.; Ananthakrishnan, S.; & Ravichandiran, P., *J Inorg Organomet.*, **2024**, 34(2), 584-592.
3. Kanagamani, K.; Muthukrishnan, P.; Ilayaraja, M.; Shankar, K.; & Kathiresan, A., *J Inorg Organomet.*, **2018**, 28, 702-710.
4. Kanagamani, K.; Muthukrishnan, P.; Shankar, K.; Kathiresan, A.; Barabadi, H.; & Saravanan, M., *J. Clust. Sci.*, **2019**, 30(6), 1415-1424.

5. Kanagamani, K.; Muthukrishnan, P.; Ilayaraja, M.; Kumar, J. V.; Shankar, K.; & Kathiresan, A., *J Photochem Photobiol A Chem.*, **2017**, *346*, 470-478.
6. Panneerselvi, V.; Shankar, K.; Muthukrishnan, P.; & Prabhu, A., *J. Clust. Sci.*, **2022**, 1-11.
7. Kumar, A.; Negi, Y. S.; Bhardwaj, N. K.; & Choudhary, V., *Carbohydr. Polym.*, **2012**, *88*(4), 1364-1372.
8. Azizi, S.; Ahmad, M.; Mahdavi, M.; & Abdolmohammadi, S., *BioResources.*, **2013**, *8*(2), 1841-1851.
9. Zhang, Y.; R Nayak, T.; Hong, H.; & Cai, W., *Curr. Mol. Med.*, **2013**, *13*(10), 1633-1645.
10. El-Hadi, A. M., *Sci. Rep.*, **2017**, *7*(1), 46767.
11. Wang, N.; Ding, E.; & Cheng, R., *Polymer.*, **2007**, *48*(12), 3486-3493.
12. Lu, P.; & Hsieh, Y. L., *Carbohydr. Polym.*, **2010**, *82*(2), 329-336.
13. Kaushik, M.; Frascini, C.; Chauve, G.; Putaux, J. L.; & Moores, A., *The Transmission Electron Microscope-theory and Applications.*, **2015**, 130-163.
14. Kwabena, E.; Droepenu & Siong, W. B.; & Chin, S.; & Kuan, Y.; & Kok, & Asare, E. A., *Biointerface Res. Appl. Chem.*, **2020**, *10*.
15. Azizan, A.; Samsudin, A. A.; Shamshul Baharin, M. B.; Dzulkiflee, M. H.; Rosli, N. R.; Abu Bakar, N. F.; & Adlim, M., *Environ. Sci. Pollut. Res.*, **2023**, *30*(7), 16779-16796.
16. Ruba, A. A.; Johnny, L. M.; Jothi, N. N.; & Sagayaraj, P., *Mater. Today: Proc.*, **2019**, *8*, 94-98.
17. Samy, A.; El-Sherbiny, A. E.; & Menazea, A. A., *Egypt. J. Chem.*, **2019**, *62*, 29-37.
18. Thipchai, P.; Punyodom, W.; Jantanasakulwong, K.; Thanakkasaranee, S.; Hinmo, S.; Pratinthong, K.; & Rachtanapun, P., *Polymers.*, **2023**, *15*(12), 2622.
19. Bodade, A. B.; Taiwade, M. A.; & Chaudhari, G. N., *J. Appl. Pharm. Res.*, **2017**, *5*(1), 30-39.
20. He, Q.; Bai, Y.; Lu, Y.; Cui, B.; Huang, Z.; Yang, Q.; & Shao, D., *Biomass Convers. Biorefin.*, **2022**, 1-10.
21. Thakur, M.; Sharma, A.; Ahlawat, V.; Bhattacharya, M.; & Goswami, S., *Mater. Sci. Energy Technol.*, **2020**, *3*, 328-334.
22. Zhou, Z.; Lu, C.; Wu, X.; & Zhang, X., *RSC Adv.*, **2013**, *3*(48), 26066-26073.
23. Ul-Islam, M.; Khattak, W. A.; Ullah, M. W.; Khan, S.; & Park, J. K., *Cellulose.*, **2014**, *21*, 433-447.
24. Zheng, Y.; Yang, J.; Zheng, W.; Wang, X.; Xiang, C.; Tang, L.; & Wang, H., *Mater. Sci. Eng. C.*, **2013**, *33*(4), 2407-2412.
25. Wahid, F.; Duan, Y. X.; Hu, X. H.; Chu, L. Q.; Jia, S. R.; Cui, J. D.; & Zhong, C., *Int. J. Biol. Macromol.*, **2019**, *132*, 692-700.
26. Janpetch, N.; Saito, N.; & Rujiravanit, R., *Carbohydr. Polym.*, **2016**, *148*, 335-344.
27. Podrojková, N.; Patera, J.; Popescu, R.; Škoviera, J.; Oriaková, R.; & Oriaková, A., *Chemistry Select.*, **2021**, *6*(17), 4256-4264.
28. Huang, S.; Zhou, L.; Li, M. C.; Wu, Q.; & Zhou, D., *Materials.*, **2017**, *10*(1), 80.